Reactions of $CH_2(\tilde{X}^3B_1)$ and $CH_2(\tilde{a}^1A_1)$ with O_2 studied by time-resolved FTIR spectroscopy

Hongmei Su, Wentao Mao, Fanao Kong *

Institute of Chemistry, Chinese Academy of Sciences, Laboratory of Molecular Reaction Dynamics, Beijing 100080, China

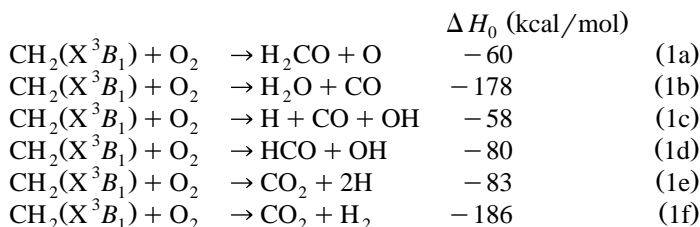Received 15 December 1999; in final form 8 March 2000

Abstract

Electronic state-specific CH_2 reactions with O_2 in the gas phase were investigated by time-resolved Fourier transform infrared emission spectroscopy. $CH_2(\tilde{X}^3B_1)$ and $CH_2(\tilde{a}^1A_1)$ radicals were produced by laser photolysis of ketene at 351 and 308 nm, respectively. Vibrationally excited products of $CO(v \leqslant 10)$, $CO_2(\nu_3, v \leqslant 7)$, $H_2CO(\nu_1)$ and $H_2O(\nu_3)$ formed in the $CH_2(\tilde{X}^3B_1) + O_2$ reaction and $CO(v \leqslant 10)$, $CO_2(\nu_3, v \leqslant 8)$, $H_2CO(\nu_1)$ formed in the $CH_2(\tilde{a}^1A_1) + O_2$ reaction have been observed. For each reaction, three possible channels have been verified. © 2000 Elsevier Science B.V. All rights reserved.

1. Introduction

The reaction of CH_2 with O_2 is one of the most important reactions in the combustion of unsaturated hydrocarbons [1–3]. Most of the previous investigations dealt with the reaction of the ground state $CH_2(\tilde{X}^3B_1)$ with O_2. Thermodynamically allowed reaction channels are the following:

$$\begin{array}{lll} & \Delta H_0 \text{ (kcal/mol)} & \\ CH_2(X^3B_1) + O_2 \rightarrow H_2CO + O & -60 & \text{(1a)} \\ CH_2(X^3B_1) + O_2 \rightarrow H_2O + CO & -178 & \text{(1b)} \\ CH_2(X^3B_1) + O_2 \rightarrow H + CO + OH & -58 & \text{(1c)} \\ CH_2(X^3B_1) + O_2 \rightarrow HCO + OH & -80 & \text{(1d)} \\ CH_2(X^3B_1) + O_2 \rightarrow CO_2 + 2H & -83 & \text{(1e)} \\ CH_2(X^3B_1) + O_2 \rightarrow CO_2 + H_2 & -186 & \text{(1f)} \end{array}$$

Wagner et al. observed the OH radical by LMR, and H and O atoms by ESR [4,5]. They also detected the transient IR emissions of CO and CO_2 in a shock tube [6]. Alvarez and Moore [3] observed CO, CO_2 and H_2CO with the time-resolved IR absorption technique. Lin et al. reported that the CO product was vibrationally excited up to $v = 13$ [7,8].

The branching ratio of the products has been estimated. The ratio of the two main products, CO/CO_2, was reported to be 4 by Wagner et al. [6] and near 1 by Moore [3]. Moore indirectly estimated the yield of OH as 30%. Wagner et al. reported that the yield of OH was only a few percent. Moore et al. also reported that 16% of the products was H_2CO.

---

* Corresponding author. Fax: +86-10-6256-3167; e-mail: kong@mrdlab.icas.ac.cn

A possible reaction mechanism with four intermediates was suggested by Moore et al. [3]:
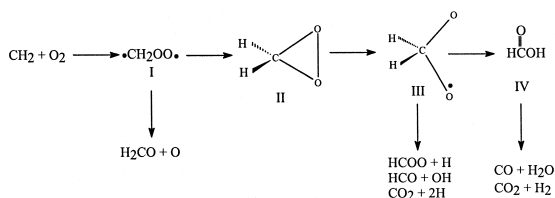
In contrast to $CH_2(\tilde{X}^3B_1) + O_2$, the reaction of the lowest excited $CH_2(\tilde{a}^1A_1)$ with O_2 has rarely been studied. The $CH_2(\tilde{a}^1A_1)$ state lies only 8.4 kcal/mol higher than the ground state $CH_2(\tilde{X}^3B_1)$ [9]. It has been reported that $CH_2(\tilde{a}^1A_1)$ is very reactive to O_2. The rate constant is 5×10^{-11} cm^3 molec^{-1} s^{-1} [10], 25 times faster than that of the $CH_2(\tilde{X}^3B_1) + O_2$ reaction (2×10^{-12} cm^3 molec^{-1} s^{-1} [11–14]). Rowland et al. [15] noted that the products from these two reactions were similar, sug-

gesting that $CH_2(\tilde{a}^1A_1)$ might be initially quenched to the ground state $CH_2(\tilde{X}^3B_1)$ and further reacted with O_2.

In this Letter, we report our investigation of state-specific reactions of both $CH_2(\tilde{X}^3B_1) + O_2$ and $CH_2(\tilde{a}^1A_1) + O_2$. It is important to compare the products of the two reactions in order to understand the mechanism. A time-resolved Fourier transform infrared (TR-FTIR) spectrometer was employed to detect products. In contrast to most previous spectroscopic detections at specific wavelengths, the TR-FTIR spectrum recorded the emissions between 1800 and 4000 cm^{-1} from the vibrationally excited products. For each reaction, three or four products were simultaneously recorded.

2. Experimental

The details of the TR-FTIR spectrometer and the reaction chamber have been described elsewhere [16].
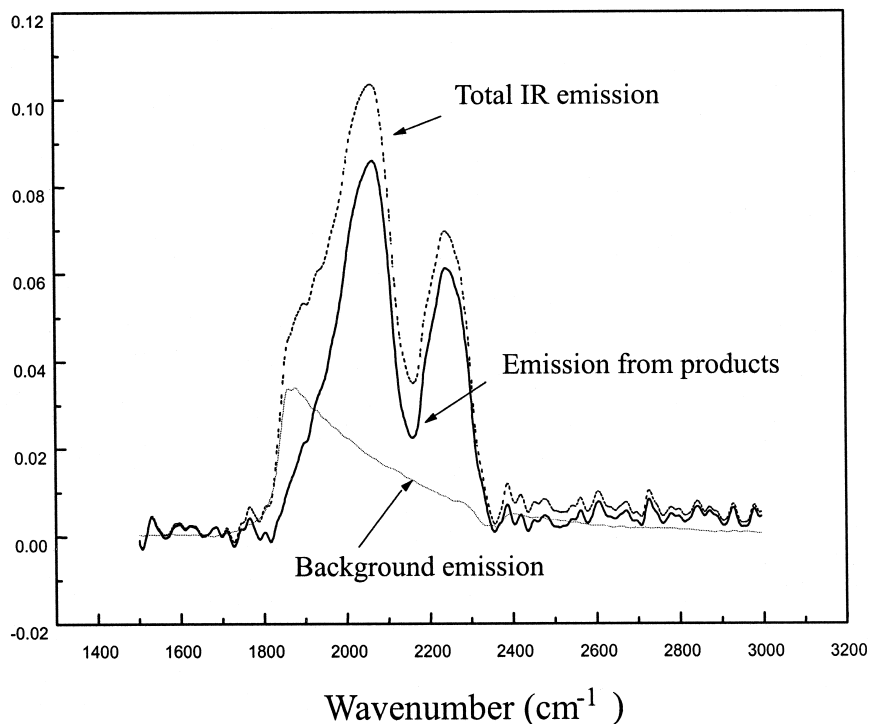

Fig. 1. The IR emission of the reaction products is obtained by subtracting the background emission from the total emission. The emission spectrum was taken at 5 μs after the XeF laser pulse fired.

$CH_2(\tilde{X}\,^3B_1)$ or $CH_2(\tilde{a}\,^1A_1)$ was produced via laser photolysis of ketene at 351 nm (XeF laser, Lambda Physik LPX 305i, $\sim$ 170 mJ/pulse) or at 308 nm (XeCl laser, Lambda Physik LPX 200, $\sim$ 80 mJ/pulse), respectively [9]. Ketene was synthesized by the pyrolysis of acetone and purified by the trap-to-trap method [17]. In the experiment, a gas mixture of 40 Pa ketene with 150 Pa O_2 flowed in the reaction chamber. The excimer laser beam was slightly focused by a cylindrical lens (f = 380 nm). The IR emisions were collected by a pair of gold-coated, confocal spherical mirrors and were collimated to the FTIR spectrometer (Nicolet 800). An InSb detector was used to detect the IR emission. The spectral resolution was set at 16 cm^{-1}. A data acquisition system provided 10 time-sequenced interferograms with 18 µs spacing.

3. Results and discussions

3.1. IR emission of the products

The CH_2 $(\tilde{X}\,^3B_1)$ radical was generated by the photolysis of ketene with a XeF laser (351 nm):

$$CH_2CO \rightarrow CH_2(\tilde{X}\,^3B_1) + CO.$$
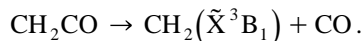
With the laser of 351 nm, the photolytic product CH_2 was ascertained in the ground electronic state $\tilde{X}\,^3B_1$ [9]. With a small amount of available energy (5 kcal/mol), the products could not be vibrationally excited. In fact, no IR emission was observed in the photolytic experiment of pure ketene. Therefore, the photolysis of ketene at 351 nm provides a neat $CH_2(\tilde{X}\,^3B_1)$ source as well as a reference IR emission background for further spectroscopic investigation.

Strong IR emission was recorded by the TR-FTIR spectrometer when O_2 was added to the above photolytic system. The reference background from the room-temperature optics has been subtracted as shown in Fig. 1. The difference is the emission spectrum of the reaction products. Fig. 2 shows the IR spectra taken at different delay times after the laser firing. Four emission bands have been observed. The band between 1820 and 2250 cm^{-1} is assigned to the vibrationally excited product $CO(v)$,
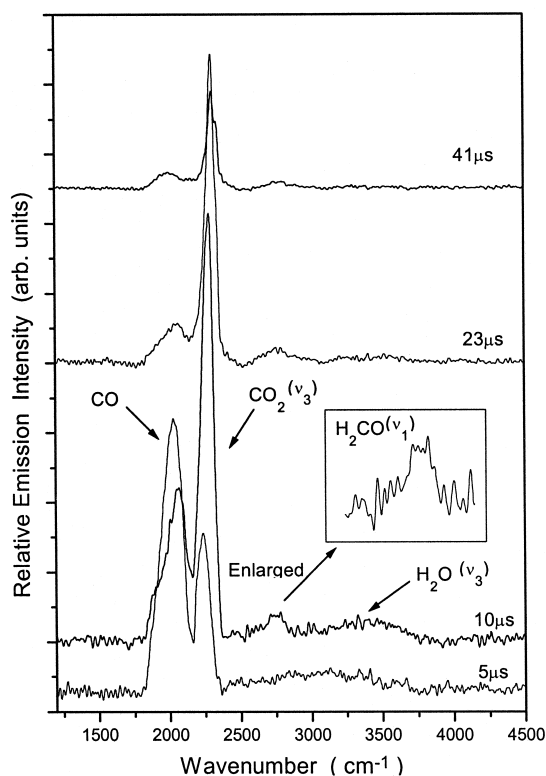

Fig. 2. IR emission spectra of the $^3CH_2O_2$ reaction products at different delay times. The inset is an enlarged H_2CO spectrum.

while that at 2130–2360 cm^{-1} is the emission of the ν_3 mode of CO_2. The band between 2500 and 2800 cm^{-1} is assigned to the ν_1 mode of H_2CO, which can be clearly seen in the insert of Fig. 2. While the band of 2800–3800 cm^{-1} may be assigned to OH or $H_2O(\nu_3)$.

$CH_2(\tilde{a}\,^1A_1)$ radical was generated by the photolysis of ketene at 308 nm [9]. No IR emission was observed after photolysis. When O_2 was added to the system, strong IR emission was observed as shown in Fig. 3. Analogous to those in the $CH_2(\tilde{X}\,^3B_1) + O_2$ reaction, three bands were recorded and also identified as CO, CO_2 and H_2CO emissions. However, a notable difference is the absence of the OH or $H_2O(\nu_3)$ band at 2800–3800 cm^{-1}.

3.2. H_2CO

Moore et al. [3] observed the IR absorption of $H_2CO(\nu_2)$ in the range of 1685–1820 cm^{-1}. We
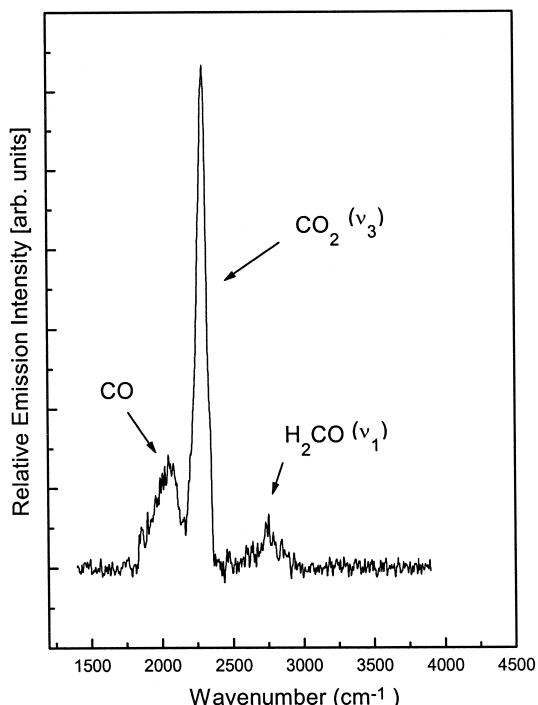
Fig. 3. IR emission spectra of the $^1CH_2 + O_2$ reaction products at a delay of 10 μs.

recorded a moderate IR emission of the ν_1 band of H_2CO (C–H symmetric stretch) at 2500–2800 cm^{-1} in both $CH_2(\tilde{X}^3B_1) + O_2$ and $CH_2(\tilde{a}^1A_1) + O_2$ reactions. The formation of H_2CO can be straightforwardly interpreted as the decomposition of the intermediate I (methylene peroxide). There is a very low energy barrier of 1.4 kcal/mol between the intermediate I and the products of H_2CO and $O(^3P)$ [3]. This reaction channel is spin-allowed for both $CH_2(\tilde{X}^3B_1) + O_2$ and $CH_2(\tilde{a}^1A_1) + O_2$ reactions. The former reaction releases 60 kcal/mol, which is sufficient for the vibrational excitation of the product H_2CO.

3.3. H_2O and OH

A broad-band emission between 2800 and 3800 cm^{-1} has been observed only in the $CH_2(\tilde{X}^3B_1) + O_2$ reaction. From 5 to 10 μs, the contour of the emission band shifts to shorter wavelength, indicating that a fast vibrational relaxation occurs. The emission may be either from the OH radical or from the ν_3 mode of the H_2O molecule. The fundamental vibrational frequencies for OH and H_2O (ν_3) are
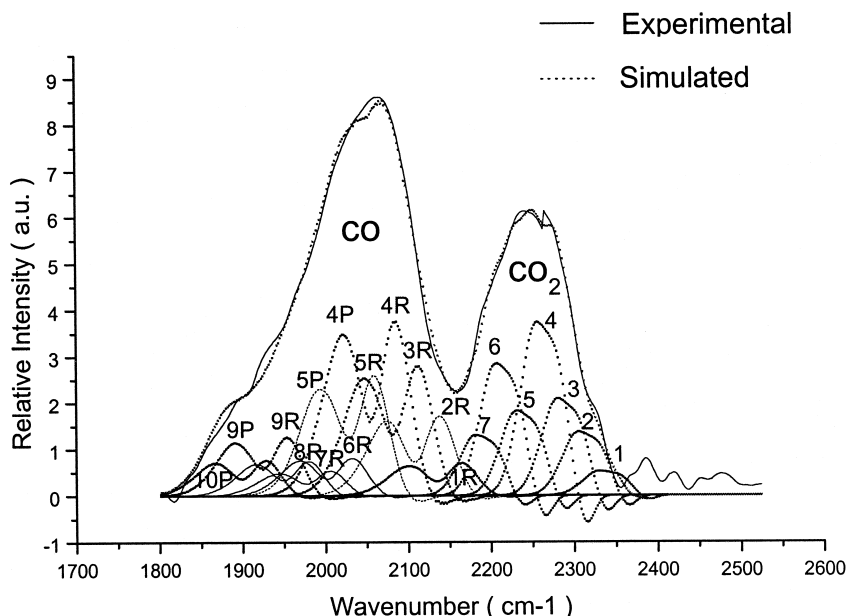

Fig. 4. The simulation of the CO and CO_2 spectra. The solid line is the experimental spectrum for the $^3CH_2 + O_2$ reaction at 5 μs. The simulated overlapping spectrum is denoted by the dotted line. Some individual ro-vibrational spectra in the simulation are also shown by the dotted lines.

Table 1
Vibrational populations of the reaction products $CO(v)$ and $CO_2(v)$

Reaction	Product	Vibrational level v								Total
		1	2	3	4	5	6	7	8	
$^3CH_2 + O_2$	CO	4.01	5.18	6.00	6.30	3.65	1.00	0.59	0.75	27.5
	CO_2	0.14	0.19	0.20	0.28	0.11	0.15	0.04		1.11
$^1CH_2 + O_2$	CO	5.82	8.28	4.69	7.87	2.03	2.16	1.33	1.69	33.9
	CO_2	0.09	0.07	0.24	0.33	0.49	0.16	0.31	0.08	1.77

3569 and 3755 cm^{-1}, respectively. Although we repeated the experiment with a better spectral resolution of 1 cm^{-1}, this emission band still could not be rotationally resolved.

3.4. CO, CO$_2$ and their vibrational populations

High vibrationally excited CO and CO_2 molecules are the main products of both reactions. The emission spectra of $CO(v)$ and $CO_2(v)$ were simulated. We made a spectral simulation program, which can fit the observed spectrum automatically. For a given rotational temperature, only the number of vibrational levels should be set. The Einstein spontaneous emission coefficients of CO and CO_2 have been used in the spectral simulation [18]. Under the pressures of 40 Pa CH_2CO and 150 Pa O_2, each CO or CO_2 molecule collides about $50 \sim 100$ times within 5 μs. Thus, the rotational distribution has been thermalized and cooled down to room temperature. We have tried different rotational temperatures in the
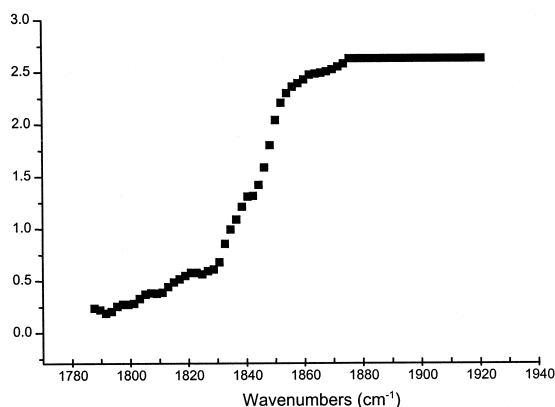

Fig. 5. The relative responses of the InSb detector to a MCT one versus wavelength are shown by the squares. The response of the MCT detector is almost constant in this wavelength region.

simulation. The best fit one was 300 K. However, in 5 μs the vibrational excitation was not relaxed remarkably. Fig. 4 shows a comparison between the experimental and the simulated spectra at 5 μs. The simulated results provide the information of the vibrational distributions of the products. It can be seen from Fig. 4 that CO is excited up to $v = 10$ and CO_2 to $v = 7$. Their vibrational populations at 5 μs are listed in Table 1. The response of the InSb detector between the wavenumbers of 1790 and 1920 cm^{-1} was measured and shown in Fig. 5. The response dramatically drops below 1860 cm^{-1}, corresponding to the P branch tail of $v = 8$ (Fig. 5). However, the nascent CO products populate mostly in the middle vibrational levels, therefore the contribution of the high levels ($v \geqslant 9$) may not be important.

The vibrational quenching of $CO(v)$ is much faster than that of $CO_2(v)$. The fast quenching is probably caused by the near resonant $v - v$ energy transfer from $CO(v)$ to the ν_2 mode of the precursor molecule CH_2CO (2152 cm^{-1}, the C–O stretching mode). Comparing to the nascent vibrational distribution ($t = 0$ μs), the population of the lowest level ($v = 1$) in Table 1 (5 μs) was overestimated.

The ratios of the total population of $CO(v)/CO_2(\nu_3, v)$ for the $CH_2(\tilde{X}^3B_1)$ and $CH_2(\tilde{a}^1A_1)$ reactions are 24.8 and 19.1, respectively (Table 1). The vibrational ground state is not included. Besides, only the bright mode, ν_3, of the CO_2 product is taken into account. Thus the true ratio of the total CO/CO_2 must be much less.

Acknowledgements

References

[1] A.H. Laufer, Rev. Chem. Intermed. 4 (1981) 225.

[2] J.A. Miller, R.J. Kee, C.K. Westbrook, Annu. Rev. Phys. Chem. 41 (1990) 345.

[3] R.A. Alvarez, C.B. Moore, J. Phys. Chem. 98 (1994) 174.

[4] U. Bley, F. Temps, H.Gg. Wagner, M. Wolf, Ber. Bunsenges. Phys. Chem. 96 (1992) 1043.

[5] Ch. Dombrowsky, S.M. Hwang, M. Rohrig, H.Gg. Wagner, Ber. Bunsenges. Phys. Chem. 96 (1992) 194.

[6] Ch. Dombrowsky, H.Gg. Wagner, Ber. Bunsenges. Phys. Chem. 96 (1992) 1048.

[7] D.S.Y. Hsu, M.C. Lin, Int. J. Chem. Kin. 9 (1997) 507.

[8] W.M. Shaub, D.S.Y. Hsu, T.L. Burks, M.C. Lin, Symp. (Int). Combust. 18th 811 (1981).

[9] C.C. Hayden, D.M. Neumark, K. Shobatake, R.K. Sparks, Y.T. Lee, J. Phys. Chem. 76 (1982) 3607.

[10] W. Tsang, R.F. Hampson, J. Phys. Chem. Ref. Data. 15 (1986) 1253.

[11] A.H. Laufer, A.M. Bass, J. Phys. Chem. 78 (1974) 1344.

[12] M.J. Pilling, J.A. Robertson, J. Chem. Soc. Faraday Trans. I 73 (1977) 968.

[13] C. Vinckier, W. Debruyn, J. Phys. Chem. 83 (1979) 2057.

[14] T. Bohland, F. Temps, H.Gg. Wagner, Ber. Bunsenges. Phys. Chem. 88 (1984) 455.

[15] F.S. Rowland, P.S.-T. Lee, C. Montague, R.L. Russell, Faraday Disc. Chem. Soc. 532 (1972) 111.

[16] Q. Zhu, S. Huang, X. Wang et al., Chin. J. Chem. Phys. 6 (1993) 87.

[17] J.T. Muckerman, J. Phys. Chem. 93 (1989) 179.

[18] H. Su, W. Feng, F. Kong, Phys. Chem. Lett., submitted.